Consistency of WIMP Dark Matter as radiative neutrino mass messenger

Alexander Merle,[a] Moritz Platscher,[b] Nicolás Rojas,[c] José W.F. Valle[c] and Avelino Vicente[c]

[a] *Max-Planck-Institut für Physik (Werner-Heisenberg-Institut),*
Föhringer Ring 6, 80805 München, Germany

[b] *Max-Planck-Institut für Kernphysik,*
Saupfercheckweg 1, 69117 Heidelberg, Germany

[c] *AHEP Group, Instituto de Física Corpuscular — C.S.I.C./Universitat de València,*
Parc Cientific de Paterna, C/Catedratico José Beltrán, 2 E-46980 Paterna (València) — Spain

E-mail: amerle@mpp.mpg.de, moritz.platscher@mpi-hd.mpg.de, nicolas.rojas@ific.uv.es, jose.valle@ific.uv.es, avelino.vicente@ific.uv.es

ABSTRACT: The scotogenic scenario provides an attractive approach to both Dark Matter and neutrino mass generation, in which the same symmetry that stabilises Dark Matter also ensures the radiative seesaw origin of neutrino mass. However the simplest scenario may suffer from inconsistencies arising from the spontaneous breaking of the underlying $\mathbb{Z}_2$ symmetry. Here we show that the singlet-triplet extension of the simplest model naturally avoids this problem due to the presence of scalar triplets neutral under the $\mathbb{Z}_2$ which affect the evolution of the couplings in the scalar sector. The scenario offers good prospects for direct WIMP Dark Matter detection through the nuclear recoil method.

Contents

1 Introduction

The popularity of the Standard Model of particle physics rests upon its enormous success in explaining weak interaction phenomena [1] in terms of weak gauge boson exchange, their explicit discovery by the UA1 and UA2 experiments [2, 3], and more recently the historic discovery of the Higgs boson [4, 5]. However, there is a number of experimental indications showing that the Standard Model must be extended. Within these experimental hints we can name two: on the one hand, the neutrino oscillations, a phenomenon that is intimately connected to neutrino masses, and on the other, the existence of a large component of Dark Matter in the Universe.

The discovery that neutrino flavours change when these particles propagate, honoured with the Nobel prize in 2015, has been confirmed in a number of independent experiments and constitutes a landmark in particle physics [6–11]. By now neutrino oscillation measurements have reached the precision era with the neutrino mixing angles and their square mass differences well determined [12].

Nevertheless, the good knowledge of the neutrino oscillation stays short of unveiling the underlying mechanism responsible for neutrino mass generation [13]. The simplest operator capable of inducing Majorana neutrino mass terms is the $d = 5$ Weinberg operator [14], which can be realised in a variety of ways in terms of heavy messenger exchange in the framework of the seesaw mechanism and its low-scale variants [15–24].

On the other hand, the standard model of cosmology indicates that most of the Universe is made up of dark stuff. In particular Dark Matter constitutes most of the total mass in the Universe, and its existence is strongly indicated by a variety of observations on smaller scales. These suggest that galaxies and galaxy clusters in the Universe as a whole contain far more matter than what is directly observable. Indeed, about 85% of the matter of the Universe is made of a type that cannot be observed via its electromagnetic coupling [25]. This is the Dark Matter problem whose ultimate physics interpretation, just like neutrino oscillations, remains a challenge.

In an attempt to understand both phenomena, it has been suggested by Ma that the smallness of neutrino mass may have its roots on the stability of Dark Matter [26], two of the major drawbacks of the Standard Model that require new particle physics. Indeed the scotogenic model is based on the validity of a $\mathbb{Z}_2$ parity symmetry which plays a double role, namely stabilising the $\mathbb{Z}_2$-odd Dark Matter particle on the one hand, and ensuring the radiative origin of neutrino mass on the other. This provides a very simple setting containing a Dark Matter candidate and generating a naturally suppressed neutrino mass at one-loop level. One of the ingredients of Ma's model is a new scalar doublet charged under the $\mathbb{Z}_2$ symmetry, similar to the inert doublet model [27]. In addition, fermion singlets are added. In both cases, future prospects in Dark Matter direct detection experiments are challenging [28].

Moreover, it has been shown that the simplest scheme suffers from a potentially severe problem, namely that loop effects [29, 30] may drive the mass parameter of the inert scalar present in the model towards negative values [31]. This behaviour would lead to the spontaneous breaking of the $\mathbb{Z}_2$ symmetry required for consistency at low energies and has thus been called the *parity problem*: without the $\mathbb{Z}_2$ parity, the model would lose its Dark Matter candidate, and the neutrino mass would no longer come from a one-loop radiative seesaw mechanism. Here we show how this problem is naturally avoided in a simple extension of Ma's idea, the singlet-triplet scotogenic model proposed in [32], partly with the aim of achieving good prospects for direct Dark Matter detection in the scotogenic scenario.

The aim of the present work is to study the $\mathbb{Z}_2$ problem of the scotogenic models within the singlet-triplet extension. We analyse in detail how the extra ingredients of the model open up the possibility of naturally preserving the $\mathbb{Z}_2$ symmetry, since the inclusion of scalar triplets neutral under the $\mathbb{Z}_2$ will change the running of the couplings in the scalar sector. Mimicking the basic features of the supersymmetry-based WIMP scenario in a simpler and realistic way, our model can ensure an adequate production of Dark Matter in the early Universe as well as sizeable Dark Matter tree-level detection rates through the nuclear recoil method. As mentioned, apart from stabilising the lightest particle odd under the $\mathbb{Z}_2$ symmetry, this provides a way to realise the Weinberg operator radiatively, giving thus a way to explain both phenomena by means of simple Standard Model extensions potentially accessible at the LHC.

The paper is organised as follows: we start in section 2 by reviewing the singlet-triplet scotogenic model, where we also make a few simplifications compared to the original reference. Our main results are presented in section 3, where we analyse the impact of the parity problem on the triplet-extended version of the scotogenic model and show how it

	Standard Model			Fermions		Scalars	
	L	e	ϕ	Σ	N	η	Ω
Generations	3	3	1	1	1	1	1
$\mathrm{SU(2)_L}$	2	1	2	3	1	2	3
$\mathrm{U(1)_Y}$	-1/2	-1	1/2	0	0	1/2	0
$\mathbb{Z}_2$	+	+	+	−	−	−	+

Table 1. Matter content and quantum numbers of the singlet-triplet scotogenic model.

can be naturally avoided in this extended setting. We finally conclude in section 4. The full set of renormalisation group equations for the singlet-triplet scotogenic model, which has been derived for the first time within this work, are listed in appendix A.

2 The model

Let us first review the singlet-triplet scotogenic model [32]. The model is based on the standard gauge symmetry $\mathrm{SU(3)_c \times SU(2)_L \times U(1)_Y}$, extended by a discrete $\mathbb{Z}_2$ parity. In addition to the Standard Model leptons and quarks, both even under $\mathbb{Z}_2$, the model contains two additional $\mathrm{SU(2)_L}$ fermion fields: the singlet N and the triplet Σ, both having vanishing hypercharge and being odd under $\mathbb{Z}_2$. The scalar sector of the model is extended as well, with the inclusion of the doublet η, also odd under $\mathbb{Z}_2$, and the real triplet Ω, even under $\mathbb{Z}_2$. The lepton and scalar sectors of the model, as well as the charge assignment under $\mathrm{SU(2)_L}$, $\mathrm{U(1)_Y}$ and $\mathbb{Z}_2$, are shown in table 1.

In this paper we will use the standard 2×2 matrix notation for the $\mathrm{SU(2)_L}$ triplets, which can (for vanishing hypercharge) be decomposed as

$$\Sigma = \begin{pmatrix} \frac{\Sigma^0}{\sqrt{2}} & \Sigma^+ \\ \Sigma^- & -\frac{\Sigma^0}{\sqrt{2}} \end{pmatrix}, \quad \Omega = \begin{pmatrix} \frac{\Omega^0}{\sqrt{2}} & \Omega^+ \\ \Omega^- & -\frac{\Omega^0}{\sqrt{2}} \end{pmatrix}. \tag{2.1}$$

The most general $\mathrm{SU(3)_c \times SU(2)_L \times U(1)_Y}$, Lorentz and $\mathbb{Z}_2$ invariant Yukawa Lagrangian is given by

$$- \mathcal{L}_Y = Y_e^{\alpha\beta} \, \overline{L_\alpha} \, \phi \, e_\beta + Y_N^\alpha \, \overline{L_\alpha} \, \tilde{\eta} \, N + Y_\Sigma^\alpha \, \overline{L_\alpha} \, \tilde{\eta} \, \Sigma + Y_\Omega \, \overline{\Sigma} \, \Omega \, N + \text{h.c.} \tag{2.2}$$

Here, gauge contractions are omitted for the sake of compactness, flavour indices $\alpha, \beta = 1, 2, 3$ are indicated explicitly, and we denote $\tilde{\eta} = i\sigma_2 \eta^*$, as usual. The Σ and N fermions are allowed to have Majorana mass terms,

$$- \mathcal{L}_M = \frac{1}{2} M_\Sigma \, \overline{\Sigma^c}\Sigma + \frac{1}{2} M_N \, \overline{N^c}N + \text{h.c.} \tag{2.3}$$

Finally, the scalar potential of the model is given by

$$\begin{aligned}
\mathcal{V} = {}& -m_\phi^2 \phi^\dagger \phi + m_\eta^2 \eta^\dagger \eta + \frac{\lambda_1}{2} \left(\phi^\dagger \phi\right)^2 + \frac{\lambda_2}{2} \left(\eta^\dagger \eta\right)^2 + \lambda_3 \left(\phi^\dagger \phi\right) \left(\eta^\dagger \eta\right) \\
& + \lambda_4 \left(\phi^\dagger \eta\right) \left(\eta^\dagger \phi\right) + \frac{\lambda_5}{2} \left[\left(\phi^\dagger \eta\right)^2 + \text{h.c.}\right] - \frac{m_\Omega^2}{2} \Omega^\dagger \Omega \\
& + \frac{\lambda_1^\Omega}{2} \left(\phi^\dagger \phi\right) \left(\Omega^\dagger \Omega\right) + \frac{\lambda_2^\Omega}{4} (\Omega^\dagger \Omega)^2 + \frac{\lambda^\eta}{2} \left(\eta^\dagger \eta\right) \left(\Omega^\dagger \Omega\right) \\
& + \mu_1 \, \phi^\dagger \, \Omega \, \phi + \mu_2 \, \eta^\dagger \, \Omega \, \eta \, .
\end{aligned} \tag{2.4}$$

Before moving on to discussing theoretical constraints on the scalar potential, we note that our notation for the Lagrangian in eqs. (2.2), (2.3), and (2.4) differs slightly from the one in ref. [32] in two ways: (i) the scalar potential has been rewritten, removing some redundant terms and renaming the remaining ones, and (ii) the normalisation of some couplings and mass terms is different. Moreover, the triplets Σ and Ω also have a different normalisation, as it is shown in the eq. (2.1).

2.1 Theoretical constraints

The couplings in the scalar potential in eq. (2.4) are subject to a number of constraints originating solely from theoretical considerations to be outlined in this subsection. First, we should ensure that the potential is bounded from below, as otherwise there is no stable minimum around which a perturbative expansion is feasible. The second constraint originates from this expansion being perturbatively valid, i.e. that the scalar quartic couplings in eq. (2.4) are $\lesssim \mathcal{O}(1)$.

In the Standard Model only a single condition is necessary and sufficient for the potential to be bounded from below, namely that the Higgs quartic coupling be positive, $\lambda > 0$. Adding a second Higgs doublet complicates the situation: simple algebraic relations that ensure the boundedness cannot be found unless further symmetry assumptions are made, e.g. an additional $\mathbb{Z}_2$ parity under which the two doublets have different quantum numbers, cf. refs. [33, 34].

Given that, in the present model, we have two scalar doublets and a triplet, finding analytic criteria for the boundedness from below of the potential is rather involved. As was noted before, the most general scalar potential allowed by the symmetries of the model contains redundant terms that have been removed in eq. (2.4) by appropriate redefinitions of the couplings $\lambda_1^\Omega, \lambda_2^\Omega, \lambda^\eta$. Consequently, the scalar potential is a function of the real and *positive* field bilinears

$$h_1^2 \equiv \phi^\dagger \phi, \quad h_2^2 \equiv \eta^\dagger \eta, \quad h_3^2 \equiv \operatorname{tr}\left[\Omega^\dagger \Omega\right]. \tag{2.5}$$

In addition, the mixed bilinear $h_{12}^2 = \eta^\dagger \phi$ can be parametrised as $h_{12}^2 = |h_1||h_2|\rho e^{i\phi}$, with $|\rho| < 1$ by virtue of the Cauchy-Schwarz inequality, $0 \leq |\eta^\dagger \phi| \leq |\eta||\phi|$.

Thus, one can write the condition of boundedness from below as

$$\mathcal{V}_4 = \left(h_1^1, h_2^2, h_3^2\right) V_4 \begin{pmatrix} h_1^2 \\ h_2^2 \\ h_3^2 \end{pmatrix} \geq 0, \tag{2.6}$$

in which the matrix of quartic couplings V_4 is given by

$$V_4 = \frac{1}{2} \begin{pmatrix} \lambda_1 & \lambda_3 + \rho^2 \left(\lambda_4 - |\lambda_5|\right) & \frac{1}{2}\lambda_1^\Omega \\ \lambda_3 + \rho^2 \left(\lambda_4 - |\lambda_5|\right) & \lambda_2 & \frac{1}{2}\lambda^\eta \\ \frac{1}{2}\lambda_1^\Omega & \frac{1}{2}\lambda^\eta & \frac{1}{2}\lambda_2^\Omega \end{pmatrix}. \tag{2.7}$$

In this expression, the phases ϕ and $\arg(\lambda_5)$ have been chosen such that the term proportional to λ_5 is minimal.[1]

---

[1]This term is given by $\frac{1}{2}\left(\lambda_5 h_{12}^4 + \lambda_5^* h_{12}^{4*}\right) = h_1^2 h_2^2 \rho^2 |\lambda_5| \cos(2\phi + \arg(\lambda_5)) \geq -h_1^2 h_2^2 \rho^2 |\lambda_5|$.

The condition $x^T V_4 x \geq 0$ for $x_i = h_i^2 \geq 0$ is known as *co-positivity* of the matrix V_4, which has been well described in ref. [35]. Using the approach outlined in this reference, necessary and sufficient conditions for the scalar potential (2.4) to be bounded from below can be obtained. In the case where $\lambda_4 + |\lambda_5| \geq 0$, we can set $\rho^2 = 0$ – the minimum of the potential as a function of ρ^2 – and in the opposite case, where $\lambda_4 + |\lambda_5| < 0$, we may fix $\rho^2 = 1$. This yields the conditions:

$$\lambda_1 \geq 0, \qquad\qquad \lambda_2 \geq 0, \qquad \lambda_2^\Omega \geq 0, \qquad (2.8\text{a})$$

$$\lambda_3 + \sqrt{\lambda_1 \lambda_2} \geq 0, \qquad\qquad \lambda_{345} + \sqrt{\lambda_1 \lambda_2} \geq 0, \qquad (2.8\text{b})$$

$$\lambda_1^\Omega + \sqrt{2\lambda_1 \lambda_2^\Omega} \geq 0, \qquad\qquad \lambda^\eta + \sqrt{2\lambda_2 \lambda_2^\Omega} \geq 0, \qquad (2.8\text{c})$$

where we have used $\lambda_{345} \equiv \lambda_3 + \lambda_4 - |\lambda_5|$. Finally, we have one more condition:

$$
\begin{aligned}
&\sqrt{2\lambda_1 \lambda_2 \lambda_2^\Omega} + \lambda_3 \sqrt{2\lambda_2^\Omega} + \lambda_1^\Omega \sqrt{\lambda_2} + \lambda^\eta \sqrt{\lambda_1} + \\
&\sqrt{\left(\lambda_3 + \sqrt{\lambda_1 \lambda_2}\right)\left(\lambda_1^\Omega + \sqrt{2\lambda_1 \lambda_2^\Omega}\right)\left(\lambda^\eta + \sqrt{2\lambda_2 \lambda_2^\Omega}\right)} \geq 0,
\end{aligned} \qquad (2.8\text{d})
$$

where — as in eq. (2.8b) — we should replace $\lambda_3 \mapsto \lambda_{345}$ in case that $\lambda_4 + |\lambda_5| < 0$.

Finally, note that considering field configurations of components of ϕ, η, or Ω will yield equivalent or redundant expressions to eqs. (2.8), because the $h_{1,2,3}^2$ are all $SU(2)_L$ invariant, as pointed out in ref. [35].[2]

2.2 Symmetry breaking

We will assume the following symmetry breaking pattern:

$$\langle \phi^0 \rangle = \frac{v_\phi}{\sqrt{2}}, \quad \langle \Omega^0 \rangle = v_\Omega, \quad \langle \eta^0 \rangle = 0, \qquad (2.9)$$

with $v_\phi, v_\Omega \neq 0$. These vacuum expectation values (VEVs) are restricted by the tadpole equations

$$t_\phi = -m_\phi^2 v_\phi + \frac{1}{2}\lambda_1 v_\phi^3 + \frac{1}{2}\lambda_1^\Omega v_\phi v_\Omega^2 - \frac{1}{\sqrt{2}} v_\phi v_\Omega \mu_1 = 0, \qquad (2.10)$$

$$t_\Omega = -m_\Omega^2 v_\Omega + \lambda_2^\Omega v_\Omega^3 + \frac{1}{2}\lambda_1^\Omega v_\phi^2 v_\Omega - \frac{1}{2\sqrt{2}} v_\phi^2 \mu_1 = 0, \qquad (2.11)$$

obtained from the scalar potential in eq. (2.4), i.e. $t_i \equiv \frac{\partial \mathcal{V}}{\partial v_i}$ is the tadpole of v_i. Given the non-trivial ϕ and Ω charges under $SU(2)_L$, the v_ϕ and v_Ω VEVs contribute to the W and Z masses,

$$m_W^2 = \frac{1}{4} g^2 \left(v_\phi^2 + 4 v_\Omega^2\right), \qquad (2.12)$$

$$m_Z^2 = \frac{1}{4} \left(g^2 + g'^2\right) v_\phi^2. \qquad (2.13)$$

---

[2]Such an approach could be useful in a case where more "unphysical" parameters such as ρ appear in the matrix V_4, as e.g. a parameter that describes the interdependence of the (in this setting redundant) operators $\mathrm{tr}\left[\left(\Omega^\dagger \Omega\right)^2\right]$ and $\mathrm{tr}\left[\left(\Omega^\dagger \Omega\right)\right]^2$, cf. ref. [36]. However, in the present situation such interdependences are absent.

We estimate that v_Ω cannot be larger than $4.5\,\mathrm{GeV}@3\sigma$ [1] in order to be compatible with electroweak precision tests, in particular those coming from the measurement of the ρ parameter.

Let us now comment on the scalar spectrum of the model. In the basis $\mathrm{Re}\left(\phi^0,\,\Omega^0\right)$ the mass matrix for the $\mathbb{Z}_2$-even and CP-even neutral scalars is given by

$$\mathcal{M}_S^2 = \begin{pmatrix} -m_\phi^2 + \frac{3}{2}\lambda_1 v_\phi^2 + \frac{1}{2}\lambda_1^\Omega v_\Omega^2 - \frac{1}{\sqrt{2}}v_\Omega\,\mu_1 & \lambda_1^\Omega v_\phi v_\Omega - \frac{1}{\sqrt{2}}v_\phi\,\mu_1 \\ \lambda_1^\Omega v_\phi v_\Omega - \frac{1}{\sqrt{2}}v_\phi\,\mu_1 & -m_\Omega^2 + \frac{1}{2}\lambda_1^\Omega v_\phi^2 + 3\lambda_2^\Omega v_\Omega^2 \end{pmatrix}. \tag{2.14}$$

The lightest of the S mass eigenstates, $S_1 \equiv h$, is identified with the $125\,\mathrm{GeV}$ state recently discovered at the LHC [4, 5]. Regarding the $\mathbb{Z}_2$-even charged scalars, their mass matrix in the basis $(\phi^\pm,\,\Omega^\pm)$ can be written as

$$\mathcal{M}_{H^\pm}^2 = \begin{pmatrix} -m_\phi^2 + \frac{1}{2}\lambda_1 v_\phi^2 + \frac{1}{2}\lambda_1^\Omega v_\Omega^2 + \frac{1}{\sqrt{2}}v_\Omega\mu_1 + \frac{1}{4}g^2 v_\phi^2 \xi_{W^\pm} & \frac{1}{\sqrt{2}}v_\phi\mu_1 - \frac{1}{2}g^2 v_\phi v_\Omega \xi_{W^\pm} \\ \frac{1}{\sqrt{2}}v_\phi\mu_1 - \frac{1}{2}g^2 v_\phi v_\Omega \xi_{W^\pm} & -m_\Omega^2 + \frac{1}{2}\lambda_1^\Omega v_\phi^2 + \lambda_2^\Omega v_\Omega^2 + g^2 v_\Omega^2 \xi_{W^\pm} \end{pmatrix}. \tag{2.15}$$

Finally, we comment on the $\mathbb{Z}_2$-odd scalars $\eta^{0,\pm}$ states. First, we decompose the neutral η^0 field in terms of its CP-even and CP-odd components as

$$\eta^0 = \frac{1}{\sqrt{2}}\left(\eta^R + i\,\eta^I\right). \tag{2.16}$$

Due to the conservation of the $\mathbb{Z}_2$ symmetry, the $\eta^{R,I,\pm}$ fields do not mix with the rest of scalars. Their masses are given by

$$m_{\eta^R}^2 = m_\eta^2 + \frac{1}{2}\left(\lambda_3 + \lambda_4 + \lambda_5\right)v_\phi^2 + \frac{1}{2}\lambda^\eta v_\Omega^2 - \frac{1}{\sqrt{2}}v_\Omega\,\mu_2, \tag{2.17}$$

$$m_{\eta^I}^2 = m_\eta^2 + \frac{1}{2}\left(\lambda_3 + \lambda_4 - \lambda_5\right)v_\phi^2 + \frac{1}{2}\lambda^\eta v_\Omega^2 - \frac{1}{\sqrt{2}}v_\Omega\,\mu_2, \tag{2.18}$$

$$m_{\eta^\pm}^2 = m_\eta^2 + \frac{1}{2}\lambda_3 v_\phi^2 + \frac{1}{2}\lambda^\eta v_\Omega^2 + \frac{1}{\sqrt{2}}v_\Omega\,\mu_2. \tag{2.19}$$

We note that the mass difference $m_{\eta^R}^2 - m_{\eta^I}^2 = \lambda_5\,v_\phi^2$ is controlled by the λ_5 coupling and vanishes for $\lambda_5 = 0$. In this limit lepton number is recovered making the neutrinos massless, as shown below.

Finally, we emphasise that the vacuum in eq. (2.9) preserves the $\mathbb{Z}_2$ scotogenic parity. This implies the existence of a stable neutral particle which can play the role of the Dark Matter of the Universe.

2.3 Neutrino masses

The $\mathbb{Z}_2$-odd fields Σ^0 and N get mixed by the Yukawa coupling Y_Ω and the triplet VEV, v_Ω. In the basis $\left(\Sigma^0, N\right)$, their 2×2 Majorana mass matrix takes the form

$$\mathcal{M}_\chi = \begin{pmatrix} M_\Sigma & Y_\Omega v_\Omega \\ Y_\Omega v_\Omega & M_N \end{pmatrix}. \tag{2.20}$$
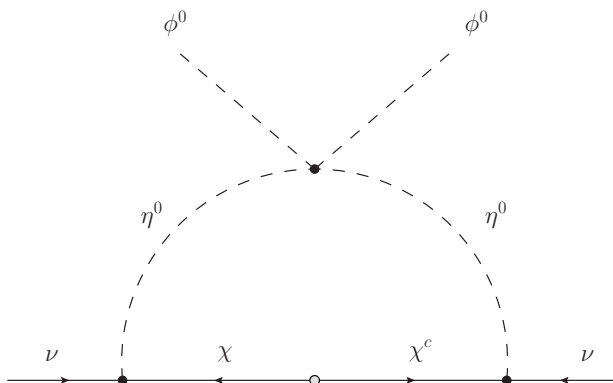
Figure 1. 1-loop neutrino mass in the singlet-triplet scotogenic model. Here $\eta^0 \equiv \left(\eta^R, \eta^I\right)$ and $\chi \equiv (\chi_1, \chi_2)$.

The mass eigenstates $\chi_{1,2}$ are obtained after rotating to the mass basis via the 2×2 orthogonal matrix $V(\alpha)$,

$$
\begin{pmatrix} \chi_1 \\ \chi_2 \end{pmatrix} = \begin{pmatrix} \cos\alpha & \sin\alpha \\ -\sin\alpha & \cos\alpha \end{pmatrix} \begin{pmatrix} \Sigma^0 \\ N \end{pmatrix} = V(\alpha) \begin{pmatrix} \Sigma^0 \\ N \end{pmatrix}, \tag{2.21}
$$

such that

$$
\tan(2\alpha) = \frac{2\,Y_\Omega v_\Omega}{M_\Sigma - M_N}\,. \tag{2.22}
$$

The singlet-triplet scotogenic model generates neutrino masses at the 1-loop level, as shown in figure 1. We emphasise that this figure actually includes four 1-loop diagrams, since $\eta^0 \equiv \left(\eta^R, \eta^I\right)$ and $\chi \equiv (\chi_1, \chi_2)$. The resulting neutrino mass matrix can be written as[3]

$$
\begin{aligned}
(\mathcal{M}_\nu)_{\alpha\beta} &= \sum_{\sigma=1}^{2} \left(\frac{ih_{\alpha\sigma}}{\sqrt{2}}\right) \left(\frac{-ih_{\beta\sigma}}{\sqrt{2}}\right) \left[I\left(M_{\chi_\sigma}^2, m_{\eta^R}^2\right) - I\left(M_{\chi_\sigma}^2, m_{\eta^I}^2\right) \right] \\
&= \sum_{\sigma=1}^{2} \frac{h_{\alpha\sigma}\, h_{\beta\sigma}\, M_{\chi_\sigma}}{2\,(4\pi)^2} \left[\frac{m_{\eta^R}^2 \ln\left(\frac{M_{\chi_\sigma}^2}{m_{\eta^R}^2}\right)}{M_{\chi_\sigma}^2 - m_{\eta^R}^2} - \frac{m_{\eta^I}^2 \ln\left(\frac{M_{\chi_\sigma}^2}{m_{\eta^I}^2}\right)}{M_{\chi_\sigma}^2 - m_{\eta^I}^2} \right],
\end{aligned} \tag{2.23}
$$

where h is a 3×2 matrix defined as

$$
h = \begin{pmatrix} \frac{Y_\Sigma^1}{\sqrt{2}} & Y_N^1 \\ \frac{Y_\Sigma^2}{\sqrt{2}} & Y_N^2 \\ \frac{Y_\Sigma^3}{\sqrt{2}} & Y_N^3 \end{pmatrix} \cdot V^T(\alpha)\,, \tag{2.24}
$$

and $I(m_1^2, m_2^2)$ is a Passarino-Veltman function evaluated in the limit of zero external momentum. We note that $m_{\eta^R}^2 = m_{\eta^I}^2$ leads to vanishing neutrino masses due to an exact cancellation between the η^R and η^I loops. This was indeed expected, since the special

---

[3]We include a factor of $1/2$ that was missing in [32].
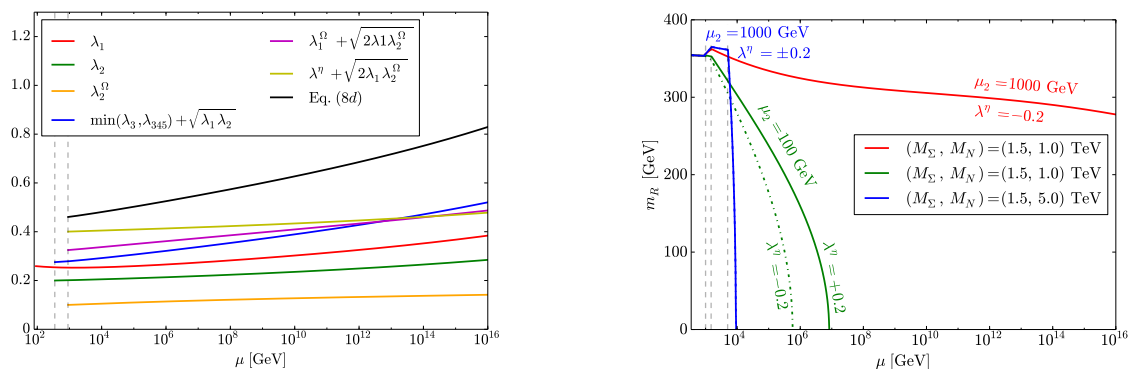
Figure 2. Running of the combinations of scalar quartic couplings relevant for the potential to be bounded from below (left panel) and of lightest inert scalar mass m_R (right panel). Vertical dashed lines are particle thresholds.

limit $m_{\eta^R}^2 = m_{\eta^I}^2$ is equivalent to $\lambda_5 = 0$, in which case one can define a conserved lepton number. As a consequence of this, the choice $\lambda_5 \ll 1$ becomes natural in the sense of 't Hooft [37], since the limit $\lambda_5 \to 0$ enhances the symmetry of the model.

3 Numerical analysis

We now discuss the running of the model parameters numerically, where we closely follow the approach of ref. [31]. The reader is referred to this reference concerning the technical details.

First, we would like to direct the readers attention to figure 2, where the running of the conditions (2.8) (left panel) and the lightest inert scalar mass parameter (right panel) is shown. The different colours in the right panel correspond to different values of fermion masses as indicated in the plot, where a scalar triplet mass parameter $m_\Omega^2 = -(900\,\text{GeV})^2$ has been chosen. Here, a negative m_Ω^2 is required by virtue of the tadpole equation (2.11): since we must have $v_\Omega \ll v_\phi$, either $\lambda_{1,2}^\Omega$ need to be very large, making the setting non-perturbative, or m_Ω^2 and/or μ_1 must be negative to solve the tadpole equation. However, applying the tadpole equations to the charged scalar mass matrix, we find that the physical charged Higgs mass $m_{H^\pm}^2 \sim \frac{\mu_1}{v_\Omega}$, and thus $\mu_1 > 0$ is required. Consequently, we need $m_\Omega^2 < 0$ to realise large triplet masses. In addition, we have verified that the conditions (2.8) are never violated for the examples shown. As an illustration, the left panel of figure 2 shows the running of the bounded-from-below conditions, see eqs. (2.8), for one of the settings in the right panel (solid green line).

It can be concluded from figure 2 that the situation is similar to the simplest scotogenic model in the sense that, once the heavy fermions become dynamic (i.e., above the renormalisation scale $\mu \geq M_{\Sigma/N}$), the RGEs of the inert mass m_R contain large and negative terms that may eventually drive m_R^2 to negative values and induce $\mathbb{Z}_2$ breaking, cf. the last two terms in eq. (A.24):

$$\beta_{m_\eta^2} \sim -3\lambda^\eta m_\Omega^2 + 3\mu_2^2 + 2\left(m_\eta^2 - 2|M_N|^2\right)\left(Y_N Y_N^*\right) + 3\left(m_\eta^2 - 2|M_\Sigma|^2\right)\left(Y_\Sigma Y_\Sigma^*\right). \quad (3.1)$$
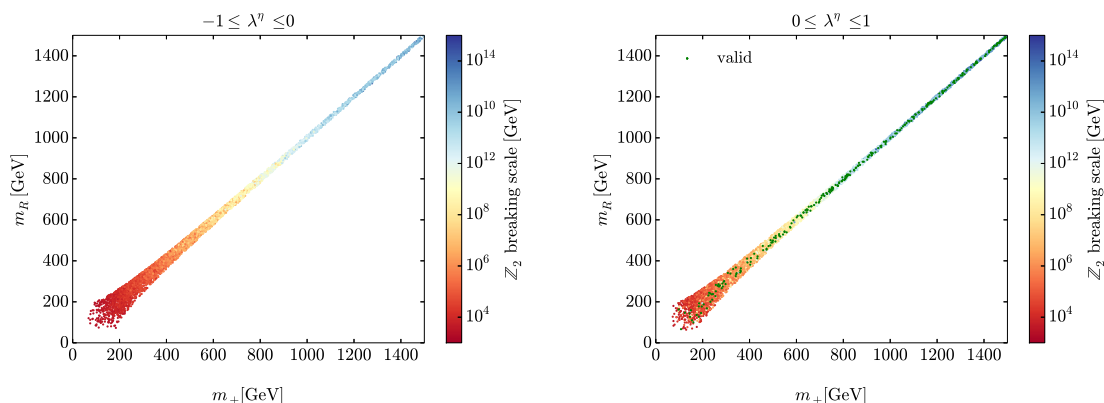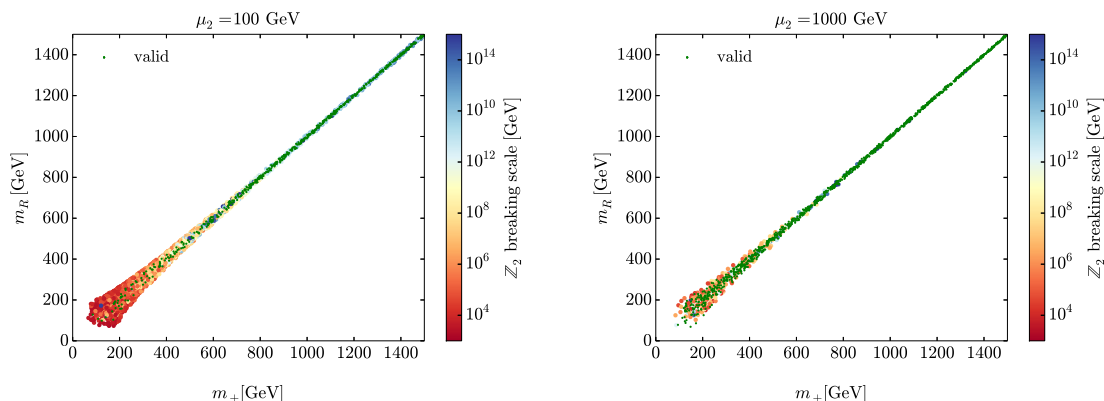
Figure 3. Parameter scan of the model for different ranges of λ^η.

Exactly that behaviour is the reflection of the parity problem in the singlet-triplet scotogenic model. However, there is a substantial difference with respect to the simplest scotogenic scenario, namely the presence of a scalar triplet field Ω which can counteract this effect. The interplay of fermion and scalar masses is manifest in the RGE (A.24), where in addition to the (generically negative) fermionic contributions, there are other contributions such as $\beta_{m_\eta^2} \sim -3\lambda^\eta m_\Omega^2$. Depending on the sign of this contribution the breaking of $\mathbb{Z}_2$ can occur at higher scales or can be evaded all together. This behaviour can be clearly observed for the green curves in figure 2, but the effect is limited if λ^η is restricted to magnitudes in the perturbative regime. More importantly, the dimensionful triple scalar couplings $\mu_{1,2}$ yield potentially large and *positive* contributions to eq. (3.1). The relevant term for the running of the inert scalar masses reads $\beta_{m_\eta^2} \sim +3\mu_2^2$. For a sufficiently large μ_2, this contribution can outweigh that of the fermions N and Σ, such that the scheme can remain consistent up to very high scales, as illustrated by the red curve in figure 2. Note that even though we have increased μ_2 significantly, the effect on the physical mass is negligible. This is due to the fact that μ_2 enters the relation for the physical masses (2.17)–(2.19) multiplied by v_Ω, which is forced to be very small. Finally, if the fermionic contributions dominate, as for the blue curve with $M_N = 5\,\text{TeV}$, the scalar contributions are practically irrelevant.

In order to better understand the impact of the running effects on the parameter space, we show in figure 3 a parameter scan of the model in the m_{η^R}-$m_{\eta^\pm}$ plane. To this end, we have chosen to fix the following parameters:

$$M_\Sigma = 1.5\,\text{TeV}, \ M_N = 2.0\,\text{TeV}, \ \lambda_2 = 0.2, \ \lambda_5 = 10^{-9}, \ Y_\Omega = 0.3, \tag{3.2}$$

while m_ϕ, λ_1, and μ_1 are fixed by the tadpole equations for $v_\Omega = 0.5\,\text{GeV}$, and the requirement of finding a 125 GeV CP-even scalar in the spectrum, which is identified with the Higgs boson. The Yukawa couplings Y_N and Y_Σ are chosen according to an adapted Casas-Ibarra-parametrisation [38] for one massless generation of neutrinos. The remaining

Figure 4. Parameter scan of the model for $\mu_2 = 100\,\text{GeV}$ and $\mu_2 = 1\,\text{TeV}$.

parameters are varied in the following ranges generating a total of $50\,000$ points:

$$(100\,\text{GeV})^2 \le m_\eta^2 \le (1500\,\text{GeV})^2, \qquad -(1500\,\text{GeV})^2 \le m_\Omega^2 \le -(500\,\text{GeV})^2,$$
$$-1 \le \lambda_3, \lambda_4, \lambda_1^\Omega \le 1, \qquad 0 \le \lambda_2^\Omega \le 1, \qquad 0 \le \mu_2 \le 100\,\text{GeV}.$$

For this set of parameters, the resulting Yukawa couplings are of the order of $\sim 10^{-1}$. The range of λ^η has been chosen differently for the left and right panels of figure 3, as given above each figure. We terminate the running at a scale $\Lambda = 10^{16}\,\text{GeV}$, motivated by theories of grand unification. However, this is a merely practical choice and just as good as any other high scale, since no gauge coupling unification is required in this model. Any parameter point that runs up to this scale is considered valid and marked as a green point. Parameter combinations violating the bounded from below conditions (2.8) or perturbativity are excluded from the plot. The remaining points indicate the breaking of $\mathbb{Z}_2$ and the corresponding scale at which the breaking occurs is displayed with a colour scale.

Quite generally, we see from figure 3 that the $\mathbb{Z}_2$ breaking scale rises with the inert masses, as expected. However, due to the large parameter space, the variation of the breaking scale for a given combination of masses is sizeable. Most notably, we see that, if $\lambda^\eta > 0$, we are able to find many viable settings for almost all values of the masses $m_{\eta R}$ and $m_{\eta \pm}$. In contrast, restricting λ^η to negative values *no* viable setting is found. The reason for this is that the breaking scale of $\mathbb{Z}_2$ is now generally lowered by the scalar triplet contribution to the running of m_η^2, as highlighted in figure 2.

Similarly, glancing at figure 4 where we keep μ_2 fixed and vary $-1 \le \lambda^\eta \le 1$ at the input scale, one observes that the impact of very large μ_2 is as anticipated. For $\mu_2 = 100\,\text{GeV}$ (left panel), $\mathbb{Z}_2$ breaking occurs for most of the points with inert scalar masses $\lesssim 500\,\text{GeV}$. However, for $\mu_2 = 1\,\text{TeV}$ most of the points turn out to be valid, even for such low scalar masses.[4] Simultaneously, the overall scalar mass scale is unchanged due to μ_2 entering the physical masses suppressed by the small triplet VEV.

---

[4]The choice $\mu_2 = 1\,\text{TeV}$ is in fact quite natural, given that the RGE (A.22) contains the fermion masses $M_{\Sigma/N}$. We also note that large trilinear couplings are known to destabilize the scalar potential due to their negative contributions to loop induced quartic scalar couplings. However, using the results of [39] we estimate that $\mu_2 = 1\,\text{TeV}$ is a safe choice given the mass scales typically considered in our paper.

In conclusion, the coupling λ^η in combination with the mass scale of the scalar triplet, and the dimensionful scalar coupling μ_2 may counteract the typical fermionic corrections to the inert scalar masses. Thus, they are the crucial ingredients that can naturally save the model from running into inconsistencies due to the breaking of the parity symmetry and provide a motivation for the presence of additional *bosonic* degrees of freedom in scotogenic-type models.

4 Summary and discussion

In this paper we have re-visited the scotogenic scenario, as it provides a common approach to the Dark Matter and neutrino mass generation problems, in which the same symmetry that stabilises Dark Matter also ensures the radiative seesaw origin of neutrino mass. We have carefully considered the behaviour of the required $\mathbb{Z}_2$ symmetry. In contrast to the simplest scenario, we have shown how the spontaneous breaking of $\mathbb{Z}_2$ can be naturally avoided in the singlet-triplet extension of the simplest model, up to fairly large energy scales, thanks to the presence of scalar triplets neutral under the $\mathbb{Z}_2$ which affect the evolution of the couplings in the scalar sector.

The singlet-triplet scotogenic model has a rich phenomenology and can be tested in several experimental fronts. For instance, scenarios with light scotogenic states and sizable Yukawa couplings lead to observable lepton flavor violating (LFV) processes in the next round of experiments [40]. In this case, bounds from LFV searches set strong constraints, to be added to those discussed in this paper. We note, however, that the LFV observables with the most stringent bounds, such as $\mu \to e\gamma$, can be suppressed with specific parameter choices.

Finally, the scenario also offers good prospects for direct WIMP Dark Matter detection in nuclear recoil experiments, in ways quite analogous to supersymmetric Dark Matter stabilised by R-parity conservation. As shown in [32], the introduction of the Ω scalar triplet not only lowers the required dark matter masses (as compared to the pure singlet or triplet scotogenic models) due to the $N - \Sigma^0$ mixing that enhances coannihilation processes, but also allows for dark matter direct detection via tree-level scalar exchange. As a consequence of this, the singlet-triplet scotogenic model produces direct detection cross-sections large enough to be observed in future experiments such as XENON1T.

A Renormalisation group equations

The β function of the parameter c, β_c, is defined by means of the renormalisation group equation

$$\frac{dc}{dt} = \beta_c = \sum_n \frac{1}{(16\pi^2)^n} \, \beta_c^{(n)} \,, \tag{A.1}$$

where $t = \log \mu$, μ being the energy scale, and $\beta_c^{(n)}$ is the n-loop β function. In this paper, we used SARAH [41, 42] to compute the β functions of all parameters in R_ξ gauge at the 1-loop level. We summarise our results here. Notice that we drop the superindex $^{(1)}$ for the sake of clarity.

A.1 Gauge couplings

$$\beta_{g_1} = \frac{21}{5} g_1^3 \tag{A.2}$$

$$\beta_{g_2} = -\frac{4}{3} g_2^3 \tag{A.3}$$

$$\beta_{g_3} = -7 g_3^3 \tag{A.4}$$

A.2 Quartic scalar couplings

$$
\begin{aligned}
\beta_{\lambda_1} =\ & +\frac{27}{100} g_1^4 + \frac{9}{10} g_1^2 g_2^2 + \frac{9}{4} g_2^4 - \frac{9}{5} g_1^2 \lambda_1 - 9 g_2^2 \lambda_1 + 12\lambda_1^2 + 4\lambda_3^2 + 4\lambda_3\lambda_4 + 2\lambda_4^2 \\
& + 2\lambda_5^2 + 3\left(\lambda_1^\Omega\right)^2 + 12\lambda_1 \mathrm{Tr}\left(Y_d Y_d^\dagger\right) + 4\lambda_1 \mathrm{Tr}\left(Y_e Y_e^\dagger\right) + 12\lambda_1 \mathrm{Tr}\left(Y_u Y_u^\dagger\right) \\
& - 12\mathrm{Tr}\left(Y_d Y_d^\dagger Y_d Y_d^\dagger\right) - 4\mathrm{Tr}\left(Y_e Y_e^\dagger Y_e Y_e^\dagger\right) - 12\mathrm{Tr}\left(Y_u Y_u^\dagger Y_u Y_u^\dagger\right)
\end{aligned} \tag{A.5}
$$

$$
\begin{aligned}
\beta_{\lambda_2} =\ & +\frac{27}{100} g_1^4 + \frac{9}{10} g_1^2 g_2^2 + \frac{9}{4} g_2^4 - \frac{9}{5} g_1^2 \lambda_2 - 9 g_2^2 \lambda_2 + 12\lambda_2^2 + 4\lambda_3^2 + 4\lambda_3\lambda_4 + 2\lambda_4^2 \\
& + 2\lambda_5^2 + 3\left(\lambda^\eta\right)^2 + 4\lambda_2\left(Y_N Y_N^*\right) - 4\left(Y_N Y_N^*\right)^2 - 4\left(Y_N Y_\Sigma^*\right)\left(Y_\Sigma Y_N^*\right) \\
& + 6\lambda_2\left(Y_\Sigma Y_\Sigma^*\right) - 5\left(Y_\Sigma Y_\Sigma^*\right)^2
\end{aligned} \tag{A.6}
$$

$$
\begin{aligned}
\beta_{\lambda_3} =\ & +\frac{27}{100} g_1^4 - \frac{9}{10} g_1^2 g_2^2 + \frac{9}{4} g_2^4 - \frac{9}{5} g_1^2 \lambda_3 - 9 g_2^2 \lambda_3 + 6\lambda_1\lambda_3 + 6\lambda_2\lambda_3 + 4\lambda_3^2 + 2\lambda_1\lambda_4 \\
& + 2\lambda_2\lambda_4 + 2\lambda_4^2 + 2\lambda_5^2 + 3\lambda_1^\Omega \lambda^\eta + 2\lambda_3\left(Y_N Y_N^*\right) - 4\left(Y_N Y_e^\dagger Y_e Y_N^*\right) + 3\lambda_3\left(Y_\Sigma Y_\Sigma^*\right) \\
& - 2\left(Y_\Sigma Y_e^\dagger Y_e Y_\Sigma^*\right) + 6\lambda_3 \mathrm{Tr}\left(Y_d Y_d^\dagger\right) + 2\lambda_3 \mathrm{Tr}\left(Y_e Y_e^\dagger\right) + 6\lambda_3 \mathrm{Tr}\left(Y_u Y_u^\dagger\right)
\end{aligned} \tag{A.7}
$$

$$
\begin{aligned}
\beta_{\lambda_4} =\ & +\frac{9}{5} g_1^2 g_2^2 - \frac{9}{5} g_1^2 \lambda_4 - 9 g_2^2 \lambda_4 + 2\lambda_1\lambda_4 + 2\lambda_2\lambda_4 + 8\lambda_3\lambda_4 + 4\lambda_4^2 + 8\lambda_5^2 + 2\lambda_4\left(Y_N Y_N^*\right) \\
& + 4\left(Y_N Y_e^\dagger Y_e Y_N^*\right) + 3\lambda_4\left(Y_\Sigma Y_\Sigma^*\right) - 2\left(Y_\Sigma Y_e^\dagger Y_e Y_\Sigma^*\right) + 6\lambda_4 \mathrm{Tr}\left(Y_d Y_d^\dagger\right) + 2\lambda_4 \mathrm{Tr}\left(Y_e Y_e^\dagger\right) \\
& + 6\lambda_4 \mathrm{Tr}\left(Y_u Y_u^\dagger\right)
\end{aligned} \tag{A.8}
$$

$$
\begin{aligned}
\beta_{\lambda_5} =\ & -\frac{9}{5} g_1^2 \lambda_5 - 9 g_2^2 \lambda_5 + 2\lambda_1\lambda_5 + 2\lambda_2\lambda_5 + 8\lambda_3\lambda_5 + 12\lambda_4\lambda_5 + 2\lambda_5\left(Y_N Y_N^*\right) + 3\lambda_5\left(Y_\Sigma Y_\Sigma^*\right) \\
& + 6\lambda_5 \mathrm{Tr}\left(Y_d Y_d^\dagger\right) + 2\lambda_5 \mathrm{Tr}\left(Y_e Y_e^\dagger\right) + 6\lambda_5 \mathrm{Tr}\left(Y_u Y_u^\dagger\right)
\end{aligned} \tag{A.9}
$$

$$
\begin{aligned}
\beta_{\lambda_1^\Omega} =\ & +3 g_2^4 - \frac{9}{10} g_1^2 \lambda_1^\Omega - \frac{33}{2} g_2^2 \lambda_1^\Omega + 6\lambda_1\lambda_1^\Omega + 4\left(\lambda_1^\Omega\right)^2 + 10\lambda_1^\Omega\lambda_2^\Omega + 4\lambda_3\lambda^\eta + 2\lambda_4\lambda^\eta \\
& + 4\lambda_1^\Omega |Y_\Omega|^2 + 6\lambda_1^\Omega \mathrm{Tr}\left(Y_d Y_d^\dagger\right) + 2\lambda_1^\Omega \mathrm{Tr}\left(Y_e Y_e^\dagger\right) + 6\lambda_1^\Omega \mathrm{Tr}\left(Y_u Y_u^\dagger\right)
\end{aligned} \tag{A.10}
$$

$$\beta_{\lambda_2^\Omega} = -24 g_2^2 \lambda_2^\Omega + 22\left(\lambda_2^\Omega\right)^2 + 6 g_2^4 + 8\lambda_2^\Omega |Y_\Omega|^2 - 8|Y_\Omega|^4 + 2\left(\lambda_1^\Omega\right)^2 + 2\left(\lambda^\eta\right)^2 \tag{A.11}$$

$$
\begin{aligned}
\beta_{\lambda^\eta} =\ & +3 g_2^4 + 4\lambda_3\lambda_1^\Omega + 2\lambda_4\lambda_1^\Omega - \frac{9}{10} g_1^2 \lambda^\eta - \frac{33}{2} g_2^2 \lambda^\eta + 6\lambda_2\lambda^\eta + 10\lambda_2^\Omega\lambda^\eta + 4\left(\lambda^\eta\right)^2 \\
& + 2\lambda^\eta\left(Y_N Y_N^*\right) + 4|Y_\Omega|^2\left(\lambda^\eta - 2\left(Y_N Y_N^*\right) - \left(Y_\Sigma Y_\Sigma^*\right)\right) + 3\lambda^\eta\left(Y_\Sigma Y_\Sigma^*\right)
\end{aligned} \tag{A.12}
$$

A.3 Yukawa couplings

$$\beta_{Y_u^{\alpha\beta}} = \frac{3}{2}\Big(Y_u Y_u^\dagger Y_u - Y_u Y_d^\dagger Y_d\Big)^{\alpha\beta}$$
$$+ \left(3\text{Tr}\Big(Y_d Y_d^\dagger\Big) + 3\text{Tr}\Big(Y_u Y_u^\dagger\Big) + \text{Tr}\Big(Y_e Y_e^\dagger\Big) - \frac{17}{20}g_1^2 - \frac{9}{4}g_2^2 - 8g_3^2\right)Y_u^{\alpha\beta} \qquad \text{(A.13)}$$

$$\beta_{Y_d^{\alpha\beta}} = \frac{3}{2}\Big(Y_d Y_d^\dagger Y_d - Y_d Y_u^\dagger Y_u\Big)^{\alpha\beta}$$
$$+ \left(3\text{Tr}\Big(Y_d Y_d^\dagger\Big) + 3\text{Tr}\Big(Y_u Y_u^\dagger\Big) + \text{Tr}\Big(Y_e Y_e^\dagger\Big) - \frac{1}{4}g_1^2 - \frac{9}{4}g_2^2 - 8g_3^2\right)Y_d^{\alpha\beta} \qquad \text{(A.14)}$$

$$\beta_{Y_e^{\alpha\beta}} = \frac{3}{2}Y_e Y_e^\dagger Y_e + \frac{1}{2}\Big(Y_e Y_N^*\Big)^\alpha Y_N^\beta + \frac{3}{4}\Big(Y_e Y_\Sigma^*\Big)^\alpha Y_\Sigma^\beta$$
$$+ \left(3\text{Tr}\Big(Y_d Y_d^\dagger\Big) + 3\text{Tr}\Big(Y_u Y_u^\dagger\Big) + \text{Tr}\Big(Y_e Y_e^\dagger\Big) - \frac{9}{4}g_1^2 - \frac{9}{4}g_2^2\right)Y_e^{\alpha\beta} \qquad \text{(A.15)}$$

$$\beta_{Y_N^\alpha} = \left(\frac{3}{2}|Y_\Omega|^2 + \frac{3}{2}\Big(Y_\Sigma Y_\Sigma^*\Big) + \frac{5}{2}\Big(Y_N Y_N^*\Big) - \frac{9}{20}g_1^2 - \frac{9}{4}g_2^2\right)Y_N^\alpha$$
$$+ \frac{1}{2}\Big(Y_e^T Y_e^* Y_N\Big)^\alpha + \frac{3}{4}\Big(Y_N Y_\Sigma^*\Big)Y_\Sigma^\alpha \qquad \text{(A.16)}$$

$$\beta_{Y_\Sigma^\alpha} = \left(\frac{1}{2}|Y_\Omega|^2 + \Big(Y_N Y_N^*\Big) + \frac{11}{4}\Big(Y_\Sigma Y_\Sigma^*\Big) - \frac{9}{20}g_1^2 - \frac{33}{4}g_2^2\right)Y_\Sigma^\alpha$$
$$+ \frac{1}{2}\Big(Y_e^T Y_e^* Y_\Sigma\Big)^\alpha + \frac{1}{2}\Big(Y_\Sigma Y_N^*\Big)Y_N^\alpha \qquad \text{(A.17)}$$

$$\beta_{Y_\Omega} = \left(6|Y_\Omega|^2 + \Big(Y_N Y_N^*\Big) + \frac{1}{2}\Big(Y_\Sigma Y_\Sigma^*\Big) - 6g_2^2\right)Y_\Omega \qquad \text{(A.18)}$$

A.4 Fermion mass terms

$$\beta_{M_N} = 2M_N\Big(Y_N Y_N^*\Big) + 3M_N|Y_\Omega|^2 + 6Y_\Omega^2 M_\Sigma^* \qquad \text{(A.19)}$$

$$\beta_{M_\Sigma} = 2Y_\Omega^2 M_N^* + M_\Sigma\Big(-12g_2^2 + |Y_\Omega|^2 + \Big(Y_\Sigma Y_\Sigma^*\Big)\Big) \qquad \text{(A.20)}$$

A.5 Trilinear scalar couplings

$$\beta_{\mu_1} = -\frac{9}{10}g_1^2\mu_1 - \frac{21}{2}g_2^2\mu_1 + 2\lambda_1\mu_1 + 4\lambda_1^\Omega\mu_1 + 2\lambda_4\mu_2 + 2\mu_1|Y_\Omega|^2 + 6\mu_1\text{Tr}\Big(Y_d Y_d^\dagger\Big)$$
$$+ 2\mu_1\text{Tr}\Big(Y_e Y_e^\dagger\Big) + 6\mu_1\text{Tr}\Big(Y_u Y_u^\dagger\Big) \qquad \text{(A.21)}$$

$$\beta_{\mu_2} = +2\lambda_4\mu_1 - \frac{9}{10}g_1^2\mu_2 - \frac{21}{2}g_2^2\mu_2 + 2\lambda_2\mu_2 + 4\lambda^\eta\mu_2 + 2\mu_2\Big(Y_N Y_N^*\Big) + 4Y_\Omega M_N^*\Big(Y_N Y_\Sigma^*\Big)$$
$$+ 4Y_\Omega M_\Sigma^*\Big(Y_\Sigma Y_N^*\Big) + 2Y_\Omega^*\Big(2M_N\Big(Y_\Sigma Y_N^*\Big) + 2M_\Sigma\Big(Y_N Y_\Sigma^*\Big) + \mu_2 Y_\Omega\Big) + 3\mu_2\Big(Y_\Sigma Y_\Sigma^*\Big) \qquad \text{(A.22)}$$

A.6 Scalar mass terms

$$
\begin{aligned}
\beta_{m_\phi^2} = & -4\lambda_3 m_\eta^2 - 2\lambda_4 m_\eta^2 - \frac{9}{10}g_1^2 m_\phi^2 - \frac{9}{2}g_2^2 m_\phi^2 + 6\lambda_1 m_\phi^2 + 3\lambda_1^\Omega m_\Omega^2 - 3\mu_1^2 + 6m_\phi^2 \mathrm{Tr}\left(Y_d Y_d^\dagger\right) \\
& + 2m_\phi^2 \mathrm{Tr}\left(Y_e Y_e^\dagger\right) + 6m_\phi^2 \mathrm{Tr}\left(Y_u Y_u^\dagger\right)
\end{aligned}
\tag{A.23}
$$

$$
\begin{aligned}
\beta_{m_\eta^2} = & -\frac{9}{10}g_1^2 m_\eta^2 - \frac{9}{2}g_2^2 m_\eta^2 + 6\lambda_2 m_\eta^2 - 4\lambda_3 m_\phi^2 - 2\lambda_4 m_\phi^2 - 3\lambda^\eta m_\Omega^2 + 3\mu_2^2 \\
& + 2\left(m_\eta^2 - 2|M_N|^2\right)\left(Y_N Y_N^*\right) + 3\left(m_\eta^2 - 2|M_\Sigma|^2\right)\left(Y_\Sigma Y_\Sigma^*\right)
\end{aligned}
\tag{A.24}
$$

$$
\begin{aligned}
\beta_{m_\Omega^2} = & -2\Big(2\lambda^\eta m_\eta^2 - 2\lambda_1^\Omega m_\phi^2 + 6g_2^2 m_\Omega^2 - 5\lambda_2^\Omega m_\Omega^2 + \mu_1^2 + \mu_2^2 - 2|Y_\Omega|^2\Big(2M_\Sigma M_\Sigma^* + m_\Omega^2\Big) \\
& - 2M_N M_\Sigma Y_\Omega^{*,2} - 2Y_\Omega M_N^*\Big(2M_N Y_\Omega^* + Y_\Omega M_\Sigma^*\Big)\Big)
\end{aligned}
\tag{A.25}
$$

Acknowledgments

References

[1] PARTICLE DATA GROUP collaboration, K.A. Olive et al., *Review of Particle Physics*, *Chin. Phys.* **C 38** (2014) 090001 [INSPIRE].

[2] UA1 collaboration, G. Arnison et al., *Experimental Observation of Isolated Large Transverse Energy Electrons with Associated Missing Energy at $\sqrt{s} = 540\,GeV$*, *Phys. Lett.* **B 122** (1983) 103 [INSPIRE].

[3] UA2 collaboration, M. Banner et al., *Observation of Single Isolated Electrons of High Transverse Momentum in Events with Missing Transverse Energy at the CERN $\bar{p}p$ Collider*, *Phys. Lett.* **B 122** (1983) 476 [INSPIRE].

[4] ATLAS collaboration, *Observation of a new particle in the search for the Standard Model Higgs boson with the ATLAS detector at the LHC*, *Phys. Lett.* **B 716** (2012) 1 [arXiv:1207.7214] [INSPIRE].

[5] CMS collaboration, *Observation of a new boson at a mass of 125 GeV with the CMS experiment at the LHC*, *Phys. Lett.* **B 716** (2012) 30 [arXiv:1207.7235] [INSPIRE].

[6] SUPER-KAMIOKANDE collaboration, Y. Fukuda et al., *Evidence for oscillation of atmospheric neutrinos*, *Phys. Rev. Lett.* **81** (1998) 1562 [`hep-ex/9807003`] [INSPIRE].

[7] SUPER-KAMIOKANDE collaboration, Y. Ashie et al., *Evidence for an oscillatory signature in atmospheric neutrino oscillation*, *Phys. Rev. Lett.* **93** (2004) 101801 [`hep-ex/0404034`] [INSPIRE].

[8] SUPER-KAMIOKANDE collaboration, S. Fukuda et al., *Determination of solar neutrino oscillation parameters using 1496 days of Super-Kamiokande I data*, *Phys. Lett.* **B 539** (2002) 179 [`hep-ex/0205075`] [INSPIRE].

[9] SNO collaboration, Q.R. Ahmad et al., *Direct evidence for neutrino flavor transformation from neutral current interactions in the Sudbury Neutrino Observatory*, *Phys. Rev. Lett.* **89** (2002) 011301 [`nucl-ex/0204008`] [INSPIRE].

[10] KAMLAND collaboration, K. Eguchi et al., *First results from KamLAND: Evidence for reactor anti-neutrino disappearance*, *Phys. Rev. Lett.* **90** (2003) 021802 [`hep-ex/0212021`] [INSPIRE].

[11] M. Maltoni, T. Schwetz, M.A. Tortola and J.W.F. Valle, *Status of global fits to neutrino oscillations*, *New J. Phys.* **6** (2004) 122 [`hep-ph/0405172`] [INSPIRE].

[12] D.V. Forero, M. Tortola and J.W.F. Valle, *Neutrino oscillations refitted*, *Phys. Rev.* **D 90** (2014) 093006 [`arXiv:1405.7540`] [INSPIRE].

[13] J.W. Valle and J.C. Romao, *Neutrinos in high energy and astroparticle physics*, John Wiley and Sons (2015).

[14] S. Weinberg, *Varieties of Baryon and Lepton Nonconservation*, *Phys. Rev.* **D 22** (1980) 1694 [INSPIRE].

[15] M. Gell-Mann, P. Ramond and R. Slansky, *Complex Spinors and Unified Theories*, print-80-0576 CERN (1979).

[16] T. Yanagida, *Horizontal Symmetry And Masses Of Neutrinos*, KEK lectures, O. Sawada and A. Sugamoto eds. (1979).

[17] R.N. Mohapatra and G. Senjanović, *Neutrino Mass and Spontaneous Parity Nonconservation*, *Phys. Rev. Lett.* **44** (1980) 912 [INSPIRE].

[18] J. Schechter and J.W.F. Valle, *Neutrino Masses in* SU(2) *x U(1) Theories*, *Phys. Rev.* **D 22** (1980) 2227 [INSPIRE].

[19] J. Schechter and J.W.F. Valle, *Neutrino Decay and Spontaneous Violation of Lepton Number*, *Phys. Rev.* **D 25** (1982) 774 [INSPIRE].

[20] G. Lazarides, Q. Shafi and C. Wetterich, *Proton Lifetime and Fermion Masses in an* SO(10) *Model*, *Nucl. Phys.* **B 181** (1981) 287 [INSPIRE].

[21] R.N. Mohapatra and J.W.F. Valle, *Neutrino Mass and Baryon Number Nonconservation in Superstring Models*, *Phys. Rev.* **D 34** (1986) 1642 [INSPIRE].

[22] E.K. Akhmedov, M. Lindner, E. Schnapka and J.W.F. Valle, *Left-right symmetry breaking in NJLS approach*, *Phys. Lett.* **B 368** (1996) 270 [`hep-ph/9507275`] [INSPIRE].

[23] E.K. Akhmedov, M. Lindner, E. Schnapka and J.W.F. Valle, *Dynamical left-right symmetry breaking*, *Phys. Rev.* **D 53** (1996) 2752 [`hep-ph/9509255`] [INSPIRE].

[24] M. Malinsky, J.C. Romao and J.W.F. Valle, *Novel supersymmetric* SO(10) *seesaw mechanism*, *Phys. Rev. Lett.* **95** (2005) 161801 [`hep-ph/0506296`] [INSPIRE].

[25] G. Bertone, D. Hooper and J. Silk, *Particle dark matter: Evidence, candidates and constraints*, *Phys. Rept.* **405** (2005) 279 [hep-ph/0404175] [inSPIRE].

[26] E. Ma, *Verifiable radiative seesaw mechanism of neutrino mass and dark matter*, *Phys. Rev.* **D 73** (2006) 077301 [hep-ph/0601225] [inSPIRE].

[27] N.G. Deshpande and E. Ma, *Pattern of Symmetry Breaking with Two Higgs Doublets*, *Phys. Rev.* **D 18** (1978) 2574 [inSPIRE].

[28] A. Ibarra, C.E. Yaguna and O. Zapata, *Direct Detection of Fermion Dark Matter in the Radiative Seesaw Model*, *Phys. Rev.* **D 93** (2016) 035012 [arXiv:1601.01163] [inSPIRE].

[29] R. Bouchand and A. Merle, *Running of Radiative Neutrino Masses: The Scotogenic Model*, *JHEP* **07** (2012) 084 [arXiv:1205.0008] [inSPIRE].

[30] A. Merle and M. Platscher, *Running of radiative neutrino masses: the scotogenic model — revisited*, *JHEP* **11** (2015) 148 [arXiv:1507.06314] [inSPIRE].

[31] A. Merle and M. Platscher, *Parity Problem of the Scotogenic Neutrino Model*, *Phys. Rev.* **D 92** (2015) 095002 [arXiv:1502.03098] [inSPIRE].

[32] M. Hirsch, R.A. Lineros, S. Morisi, J. Palacio, N. Rojas and J.W.F. Valle, *WIMP dark matter as radiative neutrino mass messenger*, *JHEP* **10** (2013) 149 [arXiv:1307.8134] [inSPIRE].

[33] M. Maniatis, A. von Manteuffel, O. Nachtmann and F. Nagel, *Stability and symmetry breaking in the general two-Higgs-doublet model*, *Eur. Phys. J.* **C 48** (2006) 805 [hep-ph/0605184] [inSPIRE].

[34] G.C. Branco, P.M. Ferreira, L. Lavoura, M.N. Rebelo, M. Sher and J.P. Silva, *Theory and phenomenology of two-Higgs-doublet models*, *Phys. Rept.* **516** (2012) 1 [arXiv:1106.0034] [inSPIRE].

[35] K. Kannike, *Vacuum Stability Conditions From Copositivity Criteria*, *Eur. Phys. J.* **C 72** (2012) 2093 [arXiv:1205.3781] [inSPIRE].

[36] J. Chakrabortty, P. Konar and T. Mondal, *Copositive Criteria and Boundedness of the Scalar Potential*, *Phys. Rev.* **D 89** (2014) 095008 [arXiv:1311.5666] [inSPIRE].

[37] G. 't Hooft, *NATO Sci. Ser.* **B 59** (1980) 135 [inSPIRE].

[38] J.A. Casas and A. Ibarra, *Oscillating neutrinos and muon → e, γ*, *Nucl. Phys.* **B 618** (2001) 171 [hep-ph/0103065] [inSPIRE].

[39] K.S. Babu and C. Macesanu, *Two loop neutrino mass generation and its experimental consequences*, *Phys. Rev.* **D 67** (2003) 073010 [hep-ph/0212058] [inSPIRE].

[40] P. Rocha-Moran and A. Vicente, *Lepton Flavor Violation in the singlet-triplet scotogenic model*, arXiv:1605.01915 [inSPIRE].

[41] F. Staub, *SARAH 4 : A tool for (not only SUSY) model builders*, *Comput. Phys. Commun.* **185** (2014) 1773 [arXiv:1309.7223] [inSPIRE].

[42] F. Staub, *Exploring new models in all detail with SARAH*, *Adv. High Energy Phys.* **2015** (2015) 840780 [arXiv:1503.04200] [inSPIRE].